A new interpretation of the necrotic changes occurring in the developing limb bud paddle of mouse embryos based upon recent observations in four different phenotypes

JEAN MILAIRE*

Department of Human Anatomy and Embryology, Faculty of Medicine, Free University of Brussels, Brussels, Belgium

ABSTRACT Degenerative changes occurring in the apical ectodermal ridge (a.e.r.) and undifferentiated distal mesoderm of developing limb buds were studied macro- and microscopically in day-11 to day-13 mouse embryos displaying the normal (+/+), oligosyndactylous (Os/+), polydactylous (Xpl/+) and hybrid (Os/+/Xpl/+) phenotypes. Isolated limb buds were submitted either to supravital staining with Nile blue sulfate or to lectin binding staining in serial paraffin sections, taking advantage of strong binding affinities of macrophage cells for peanut agglutinin after neuraminidase treatment and for ricinus communis agglutinin. Necrotic changes detected in three definite areas of the distal mesoderm of normal limb buds exhibit characteristic spatial temporal relationships with earlier cytolytic changes affecting the pre- and postaxial parts of the a.e.r. Two of them, known as the primary preaxial site *(fpp)* and the anterior marginal necrotic zone (AMNZ) appeared deeply modified in mutant embryos as compared to the posterior marginal necrotic zone (PMNZ) which remained unaffected. Macrophage cells loaded with cell debris appear in advance and in excessive number in the *fpp* of Os/+ limb buds. Conversely, they were found absent or locally reduced in number in the *fpp* and AMNZ of Xpl/+ limb buds which otherwise develop in the same area a preaxial protrusion covered with a healthy portion of the a.e.r. Hybrid Os/+/Xpl/+ limb buds expressing both mutant genes develop a smaller and macrophage-free preaxial protrusion which coexists with residual and locally excessive necrotic changes in its immediate surrounding and is covered with a normally necrotic portion of the a.e.r. Microscopic observations collected in the limb buds of all phenotypes, though more frequently in Os/+ limb buds, strongly suggest that in all three necrotic sites examined, macrophage cells of vascular origin somehow contribute to the clearance of ectodermal necrotic debris and eventually return in the blood stream through the marginal vein and its affluents.

KEY WORDS: *limb buds, necrotic sites, mouse embryo, mutant mice*

Introduction

Already mentioned in several older publications (Milaire, 1965, 1967a, 1971), the programmed degenerative phenomena detected in normal mouse and rat limb buds were first described in detail in a study focused on digital rudimentation in rodent species as compared to the digital pattern in the mole (Milaire, 1976). Three necrotic waves were demonstrated in the undifferentiated mesoderm of the early foot- and handplate of rat and mouse embryos, each with a specific spatial and chronological pattern. The first necrotic site appears in a limited preaxial area facing the anterior extremity of the apical ectodermal ridge (a.e.r.); it is known as the *fpp* site according to its french terminology *(foyer préaxial primaire)*. Two other necrotic waves occur at later stages in the marginal subridge mesoderm, one preaxially and the other postaxially; they

will be referred to as the anterior and posterior marginal necrotic zones (AMNZ and PMNZ). Interestingly, each necrotic site appeared several hours after physiological cell death had been demonstrated in the adjacent portion of the a.e.r., although the precise relationship between ectodermal and mesodermal cell death has never been elucidated.

Absence or reduction in the amount of cell debris in the *fpp* site and in the AMNZ has been reported in various induced (Scott et al.,

---

---

*Address for reprints: Université Libre de Bruxelles, Laboratoire d'Anatomie et d'Embryologie humaines, route de Lennik, 808 (C.P. 619), B-1070 Bruxelles, Belgium. FAX: 32-2-555.6378.
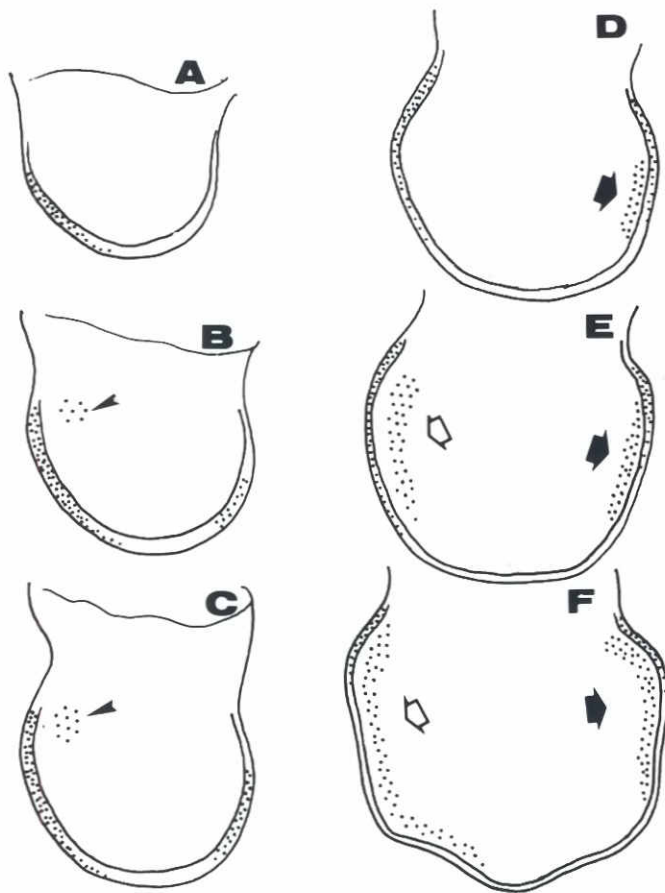
Fig. 1. Schematic distribution of cell debris in the apical ectodermal ridge and handplate mesoderm of the right forelimb bud, as demonstrated with supravital Nile blue staining (ventral views). (A,B,C,D,E,F) *Normal embryos with a CR length of 5.24, 5.84, 6.19, 7.43, 7.78 and 8.70 mm, respectively. Arrowhead: primary preaxial site or* fpp; *white arrows: anterior marginal necrotic site; black arrows: posterior marginal necrotic site.*

1977, 1980; Scott, 1981; Skalko et al., 1977; Klein et al., 1981) as well as inherited (Milaire, 1965, 1989; Naruse and Kameyama, 1986) teratological situations resulting in preaxial polydactyly or triphalangism of digit I. Conversely, excessive and advanced occurrences of cell death in the *fpp* site have been described in all limb buds of mutant mouse embryos heterozygous for the gene «Oligosyndactyly» which develop different forms of coalescence between the rudiments of digits II and III (Milaire, 1967b; Milaire and Rooze, 1983). Briefly, reduction or increase of cell death in the preaxial mesoderm has been tentatively correlated to a regional increase or reduction of cell growth, which in turn was rendered responsible for the genesis of excessive or deficient digital patterns, respectively. The fact remains, however, that the evidence provided in support of a relationship between reduced cell death and excessive digital pattern is much more convincing than that supporting the reverse situation. The prospective territory of digit I as well as its immediate preaxial surrounding where *fpp* cell death is predominant is regularly involved in the genesis of preaxial polydactyly.

In contrast, pattern formation occurs normally in the same territory of oligosyndactylous limb buds which exhibit different kinds of fusion between the 2nd and 3rd digital rays condensing more caudally with respect to the excessive *fpp*.

It was therefore interesting to combine in the same embryos two mutant genes, one responsible for oligosyndactylism and the other for preaxial polydactyly, to see what the consequences would be on the digital pattern and on the degenerative changes in the mesoderm of their prospective distal segment. This was done in the present study by mating Os/+ mice with Xpl/+ mice expressing the gene for X-linked polydactyly (Milaire, 1989). The necrotic changes occurring in developing limb buds have been studied comparatively in normal (+/+), polydactylous (Xpl/+), oligosyndactylous (Os/+) and hybrid (Os/+/Xpl/+) embryos from stage day-11 to stage day-13.

The results obtained indicate that the expression of the Xpl phenotype can be attenuated by the Os/+ condition whereas the Os phenotype was never found modified in the presence of the Xpl gene. In addition, the easy detection of macrophage cells due to selective lectin binding properties has allowed detailed observations, which led us to revise completely our interpretation of the role played by normal or abnormal cell degeneration in the genesis of the digital pattern. These include new data about the origin and fate of macrophage cells as well as about the relationship between ectodermal cell death and the appearance of macrophage cells in the underlying mesoderm.

Results

Skeletal defects observed in full-term Os/+/Xpl/+ hybrid fetuses

Among the 8 fetuses sacrificed on day 18 of gestation from a Xpl/+ female mated with a Os/+ male, 3 exhibited the Xpl/+ phenotype, 1 the Os/+ phenotype and 2 the combined Os/+/Xpl/+ phenotype. As previously reported (Grüneberg, 1961; Milaire, 1967b), the Os/+ phenotype consists of different rates of fusion between digits II and III in both hands and feet. Phalangeal fusions are regularly observed in the hindlimb with decreasing severity in proximodistal direction; complete or distal fusion of the corresponding metatarsals may be present in the more severely affected limbs, the maximal expression being a complete coalescence of metatarsals and phalanges with the external appearance of an oligosyndactylous four-toed foot. Skeletal fusions are less frequent in the forelimbs, where the coalescence between digits II and III is often restricted to soft tissues only. The Xpl/+ phenotype is characterized by the presence of extra preaxial digital parts in one or both hindlimbs, with a predominance for the left side; they vary from a single triphalangy of the first toe to as many as four extra toes on one or both feet. As described in a recent study (Milaire, 1989), the most frequent abnormal pattern is the presence of one complete extra preaxial triphalanged toe associated with triphalangy of the first toe.

Skeletal II + III syndactyly was present bilaterally in the two hybrid Os/+Xpl/+ fetuses, but only their left feet exhibited the Xpl/+ phenotype. One had the usual complete preaxial extra toe associated with a triphalanged hallux. The extra preaxial toe of the other was connected to a distal duplication of the first metatarsal, which itself was otherwise associated to a normal biphalanged hallux. Considering the limited number of hybrid embryos, it was not possible to perceive whether one genotype had influenced the expression of the other or not.

Macroscopic identification of the phenotypes in day-11 to day-13 embryos

The Os/+ phenotype could be identified from day-11 onward by a characteristic preaxial flattening of the limb bud foot- or handplate (Fig. 3A). The deficient area covers the prospective territories of the 1st and 2nd toes. In the youngest embryos of group 1, the oligosyndactylous condition could always be ascertained by the abnormal outline of the forelimb buds, even if the flattening is still imperceptible in the less advanced hindlimb buds. In age-groups 2 and 3, the type of future syndactyly could be predicted from the particular outline of the 2nd and 3rd digital buds, which exhibit various degrees of coalescence.

The Xpl/+ phenotype could be first distinguished by the presence of a localized overgrowth of preaxial subridge mesoderm in the prospective area of digit 1 or immediately anterior to it. The resulting preaxial protrusion was detected without doubt in both hindlimb buds of several embryos with a CR length superior to 6.50 mm. At later stages, the protrusion grows to variable sizes (Fig. 3B) and eventually exhibits one or more extra digital outgrowths.

In 11-day embryos with a CR length superior to 6.50 mm, the hybrid Os/+/Xpl/+ phenotype was easily identified by the presence of a typical protrusion bulging on the anterior edge of an otherwise deficient footplate displaying the preaxial flattening characteristic of the oligosyndactylous condition. In embryos of age-groups 2 and 3, the preaxial protrusion frequently appeared smaller as compared to that of Xpl/+ embryos of similar age (Fig. 3C).

Among the 65 embryos obtained from 12 matings between Xpl/+ females and Os/+ males, 16 (24.62%) were phenotypically normal, 20 (30.77%) displayed the Os/+ phenotype, 15 (23.08%) displayed the Xpl/+ phenotype and 14 (21.54%) exhibited the combined Os/+/Xpl/+ phenotype. If we consider that the Xpl condition may have escaped our attention in a few embryos with a CR length inferior to 6.50 mm, the results obtained seem to be in good agreement with the 1/4:1/4:1/4:1/4 Mendelian prediction.

Macroscopic analysis of necrotic sites detected with the Nile blue sulfate supravital staining method.

Both limb types have been examined in +/+ and Os/+ embryos, the hindlimb buds only in the embryos expressing the Xpl/+ and the Os/+/Xpl/+ phenotypes.

The normal (+/+) phenotype

From the earliest stage examined, degenerative changes could be detected in the a.e.r. of both types of limb bud; up to around the 6mm stage, they hit preferentially the whole preaxial half with a typical craniocaudal gradient of decreasing intensity (Figs. 1, 2A,B). This preaxial ectodermal cell death is still present in 9.50mm embryos (group 3) when the growing digital buds start modifying the marginal outline of the limb bud paddle (Figs. 1D,E and Fig. 2D); later on, the necrotic changes become gradually restricted to the area of the first digital bud (Figs. 1F and 2E) before being eventually shifted to a short preaxial portion of the a.e.r. located anteroproximally with respect to the first digit. A second and more discrete (Figs. 1B,C and 2B,C) necrotic site was detected in the postaxial part of the a.e.r. as soon as the limb bud paddle acquired a regular circular shape in embryos with a CR length between 6 and 7 mm. The affected ectoderm corresponds to the prospective area of digit V and of the 4th interdigital zone; it is also shifted at later stages to the extreme postaxial extremity of the ridge which covers the 5th digital bud (Figs. 1F and 2E).
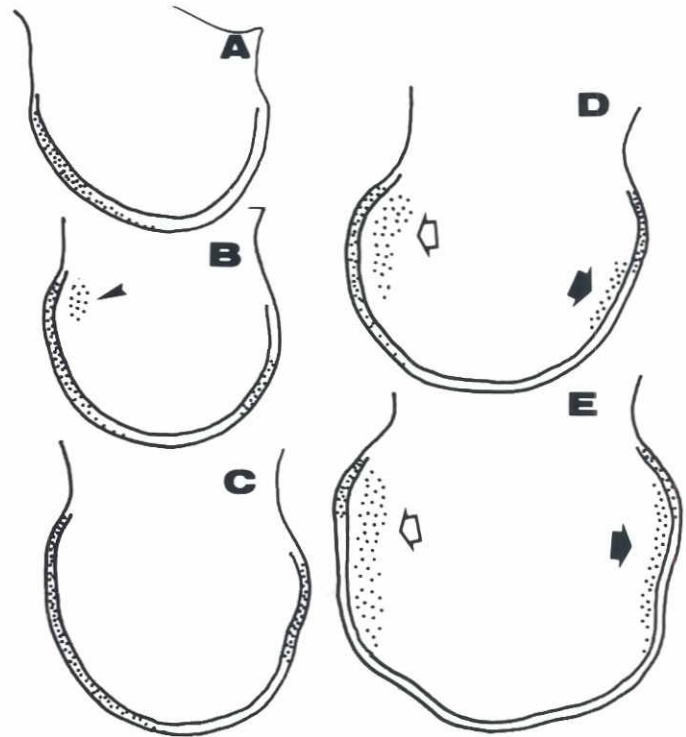

Fig. 2. Schematic distribution of cell debris in the apical ectodermal ridge and footplate mesoderm of the right hindlimb bud, as demonstrated with supravital Nile blue staining (ventral views). (A,B,C,D,E:) *Normal embryos with a CR length of 6.00, 6.86, 7.93, 8.27 and 8.76 mm, respectively. Arrowhead: primary preaxial site or fpp; white arrows: anterior marginal necrotic zone; black arrows: posterior marginal necrotic zone.*

Occurring in three waves, the degenerative changes detected in the limb paddle mesoderm display a remarkable correlation in time and area with those observed in the apical ectoderm. A first preaxial site appears around the 5.50mm stage (group 1) in the forelimb bud (Fig. 1B) and the 6.20mm stage in the hindlimb bud (Fig. 2B). This so-called *fpp (foyer préaxial primaire)* site lies in the deep mesoderm facing the strongly necrotic preaxial end of the a.e.r. Its deep location hinders its demonstration in bulk preparations, particularly in the hindlimb buds where the *fpp* vanishes more rapidly than in the forelimb buds. After a short developmental period during which the foot- and handplate mesoderm remains free of degenerative changes (Figs. 1D and 2C), a second necrotic site appears in the outer marginal mesoderm of the prospective 4th interdigital area, exactly where necrotic changes were detected a little earlier in the a.e.r. (Figs. 1D and 2D). This so-called posterior marginal necrotic zone (PMNZ) appears in the fore- and hindlimb buds of embryos with a CR length of about 7.40 and 7.90 mm respectively (group 2). As a result of its postaxial extension, the PMNZ gradually covers the area of digit V (Figs. 1F and 2D).

Occurring shortly after the PMNZ, a third necrotic wave appears in the deep mesoderm of the preaxial marginal territory. This anterior marginal necrotic zone (AMNZ) appears in the forelimb buds (Fig. 1E) of embryos with a CR length of about 7.75 mm and covers a large territory extending from the prospective area of digit
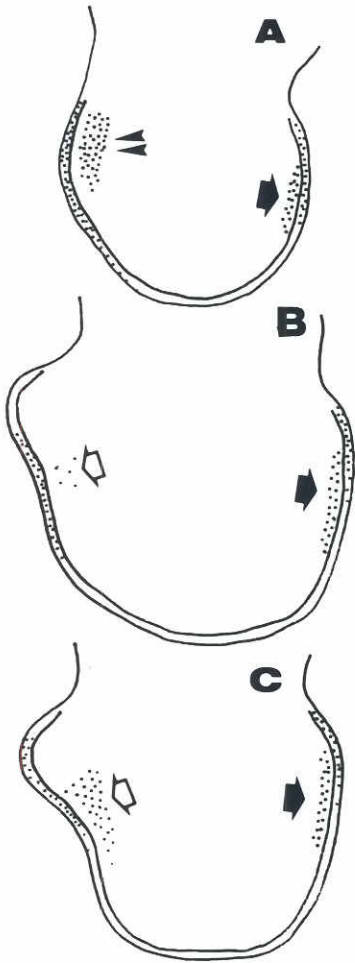
Fig. 3. Schematic distribution of cell debris in the apical ectodermal ridge and footplate mesoderm of right hindlimb buds from Os/+ (A) *8.19 mm, Xpl/+,* **(B)** *8.86 mm and Os/+/Xpl/+ (C)* *9.19 mm embryos, as demonstrated with supravital Nile blue staining (ventral views). Double arrowhead: enlarged and overcrowded primary preaxial site or fpp; white arrows: residual anterior marginal necrotic site; black arrows: posterior marginal necrotic site.*

pattern is fully established in the autopod territory. Cell death occurs according to the normal schedule and pattern in both the ectoderm and the PMNZ of Os/+ limb buds. However, the amount of cell death per surface area can hardly be assessed in the ectoderm with the staining method used.

The Xpl/+ phenotype

Necrotic material was absent in the *fpp* site and dramatically reduced in the AMNZ of 10 hindlimb buds bearing the typical preaxial protrusion and belonging to Xpl/+ embryos which did not express the Os gene. A limited number of dead cells were occasionally observed at the posterior extremity of the AMNZ area in a few limb buds with a preaxial protrusion (Fig. 3B).

It may be interesting to note that a short segment of the a.e.r. covering completely or partially the preaxial protrusion regularly remains devoid of stainable degenerative debris. Moreover, a similar preaxial unstained segment of the a.e.r. was observed unilaterally in two early embryos with a CR length of 6.19 and 6.45 mm, i.e., before the preaxial outgrowth characteristic of the Xpl/+ phenotype could be distinguished.

The hybrid Os/+Xpl/+ phenotype

Six embryos with a CR length varying from 7.02 to 9.19 mm and expressing the combined Os/+/Xpl/+ phenotype were submitted to supravital Nile blue staining. The preaxial protrusion was present bilaterally in only one case; it was found in the left hindlimb of 3 embryos and in the right hindlimb of 2 embryos. The typical Os/+ pattern of degenerative changes was found in all hindlimb buds lacking the protrusion. In protrusion-bearing limb buds, complete absence of stainable material was observed in the mesoderm of the abnormal outgrowth and in its immediate surroundings. Further posteriorly, however—i.e., in the prospective areas of the first interdigital territory and second digit—degenerative tissue was found present with the same increased density characteristic of the Os/+ phenotype (Fig. 3C). In addition, contrary to the observations in Xpl/+ embryos, the apical ectoderm covering the preaxial protrusion was always found intensely necrotic. As already mentioned above, the preaxial protrusion of hybrid embryos frequently appears smaller and wedge-shaped as compared to the large rounded overgrowth usually observed in most Xpl/+ embryos.

The distribution pattern of macrophage cells in normal and abnormal limb buds

Strong intracytoplasmic binding affinities for PNA after neuraminidase treatment (N-PNA) as well as for RCA characterize the macrophage cells, which therefore could be easily distinguished from the surrounding healthy mesodermal cells. In the ectoderm, however, and particularly in the a.e.r., similar staining properties characterize both healthy and degenerating cells so that the method is much less appropriate for studying degenerative changes in the ectodermal layer. A selective affinity of both lectins for endothelial cells also permitted a clear-cut demonstration of the vascular network. It may also be worth mentioning that early preskeletal areas of the limb bud mesoderm exhibit selective N-PNA staining which is mainly extracellular.

The observations made in serial sections of hindlimb buds displaying the different phenotypes have provided two kinds of information deserving separate descriptions. The first series of data helps give more insight into the various changes affecting the spatiotemporal pattern of macrophage distribution in each particu-

I to the preaxial border of that of digit III (Fig. 1F). In the hindlimb buds, the AMNZ (Fig. 2D) appears around the 8.25mm stage and does not extend further caudally than the middle of the second digital territory (Fig. 2E). In embryos of group 3 with a CR length superior to 10 mm, the AMNZ and PMNZ become gradually disrupted and replaced by the interdigital necrotic areas, not considered in the present study.

The Os/+ phenotype

Degenerative changes in the *fpp* site appear ahead of schedule and in increased amounts in early limb buds of the Os/+ phenotype (Fig. 3A). An obviously enlarged *fpp* was already observed in affected forelimb buds of 5.19mm embryos and in the hindlimb buds of 5.41mm embryos. At such early stages, the necrotic changes take place before any detectable reduction in the amount of preaxial mesoderm and therefore represent the only distinctive sign of the Os/+ phenotype. In both limb types, the enlarged *fpp* remains present when the preaxial flattening of the paddle becomes obvious, and it is still detectable when the later AMNZ makes its appearance. Contrary to the observations made in normal limb buds, necrotic changes thus remain continuously present in the preaxial mesoderm of Os/+ limb buds; the AMNZ eventually recovers the normal density of cell debris at the 7.50 and 9.00mm stages, respectively, in the fore- and the hindlimb buds, i.e., when the abnormal preskeletal

lar genetical condition. The second series of histological findings emphasizes more general features common to all phenotypes and which may be suggestive of the origin, fate and behavior of macrophage cells in developing limb buds.

Distribution pattern of macrophage cells in the different phenotypes

The distribution areas of macrophage cells detected in serial sections thanks to their lectin binding affinities are practically superimposable on those demonstrated macroscopically with the Nile blue sulfate staining. More details, however, were obtained concerning the *fpp* site, which, as a result of its deep location, was irregularly observed in whole-mount preparations. The presence of macrophage cells in the *fpp* site of hindlimb buds was always observed in normal embryos with a CR length between 6.50 and 7.70 mm (Fig. 4); at the same time, other macrophage cells could be demonstrated in the central area of the distal zeugopod territory, a necrotic site which probably corresponds to the avian «opaque patch» described in similar location in the chick embryo (Fig. 18). Macrophage cells of the *fpp* and AMNZ areas exhibit different topographical relationships with the marginal venous network as compared to those of the PMNZ. Small veins running in the deep mesoderm underlying the preaxial extremity of the a.e.r. assemble into a large marginal vein coursing craniocaudally and collecting on its proximal aspect numerous small radial vessels resulting from the division of the main axial artery. In many places of its preaxial course, the marginal vein comes into direct contact with the apical ectoderm (Fig. 17); such contacts were never observed postaxially where the vessel was always found separated from the a.e.r. by a relatively constant amount of distal mesoderm (Fig. 8). Contrary to those of the PMNZ which remain confined between the marginal vein and the ectoderm (Fig.8), the macrophage cells of the *fpp* and, later on, those of the AMNZ appeared scattered in a larger area including the preaxial venous network and the radial affluent vessels of the marginal vein (Figs. 4 and 7). Many macrophage cells of the *fpp* site take place inside early condensing N-PNA-positive preskeletal tissue (Fig. 4) in the prospective area of the first digit and anterior to it. Similarly, many macrophage cells of the later AMNZ were found lying within and around the distal part of the first digital column (Fig. 7).

The *fpp* of early Xpl/+ hindlimb buds was either completely absent or reduced to a few macrophage cells located on the posterior border of the preaxial protrusion (Fig. 9). At later stages, the preaxial outgrowth remained macrophage-free and only a few macrophage cells were occasionally observed close to the second digital ray, where they obviously represent the posterior extension of the AMNZ (Fig. 10).

In contrast, a striking increase in the number of macrophage cells was noted in the *fpp* site of Os/+ limb buds (Fig. 11) and, up to the 10mm stage, their excess number remained clearly perceptible in the preaxial part of the later AMNZ (Fig. 12).

The increased macrophage cell number characteristic of Os/+ limb buds was also obvious in those Os/+/Xpl/+ hybrid hindlimb buds bearing a preaxial protrusion. They were found here in the mesoderm adjacent to the base or to the posterior margin of the preaxial outgrowth (Figs. 14,15,16).

More general features suggestive of the origin and behavior of macrophage cells

Neither the macroscopic analysis using the supravital Nile blue staining nor the microscopic demonstration of lectin binding sites in serial sections provided any information on the identity and location of the dying cells prior to their eventual phagocytic removal. Our lectin binding study has, however, provided several pieces of information that might afford new insight into the problem of the origin and fate of macrophage cells detected in the marginal mesoderm.

The first and probably the most intriguing observation was the early appearance of a great number of N-PNA and RCA strongly positive blood cells in the small divisions of the axial artery (Figs. 5 and 6). They are larger than erythroblasts, their strong staining affinity is uniformly distributed in the cytoplasm and many of them appear binucleated (Figs 5 and 6); their presence in the limb buds of all phenotypes was particularly obvious in embryos with a CR length varying from 7 to 8 mm, i.e., when degenerative signs are about to occur in the marginal territory.

Macrophage cells loaded with strongly stained phagocytic inclusions display the same size as the aforementioned positive blood cells and at least some of them contained two nuclei (Fig. 18); the number of nuclei may, however, be difficult to distinguish in paraffin sections in which the cells are differently oriented and many of them are partially amputated. The mesodermal cells surrounding macrophage cells in the so-called «necrotic area» appeared healthy both after lectin staining and after Pyronin-Methyl green staining. Several macrophage cells displaying similar histochemical and cytochemical features were observed inside the marginal vein or in one of its preaxial divisions (Fig. 17). The number of intravascular macrophage cells was significantly higher in limb buds exhibiting the Os/+ phenotype. It was also in Os/+ limb buds that numerous macrophage cells were found aligned in close contact with the basement membrane underlying the preaxial part of the a.e.r. adjacent to the *fpp* and AMNZ (Fig. 13). Single subectodermal macrophage cells were occasionally observed in the preaxial territory of normal limb buds, as well as in the postaxial area facing the PMNZ in all phenotypes (Fig. 8).

These observations suggest that circulating macrophage cells leave the vascular network in the vicinity of the necrotic portions of the apical ectodermal ridge, somehow help remove ectodermal necrotic debris, migrate for a while in the underlying mesoderm and eventually return in the blood stream through the marginal vein. The extent to which this new concept may shed more light on the mechanisms involved in the genesis of the Os/+, Xpl/+ and Os/+/Xpl/+ phenotypes will be considered in the discussion.

Discussion

As stated by Hinchliffe (1981) in his extensive survey on cell death in embryogenesis, we understand better the extrinsic control of developmental cell death than the self-destruct mechanism itself. From studies on mesenchymal cell death in chick limb buds, however, a picture emerges according to which programmed cell degeneration would share some resemblance with the «autophagic» type of cell death, a variant of apoptosis (Wyllie et al., 1980) as described by Schweichel and Merker (1973) and later reviewed by Clarke (1990). The following sequence of events was suggested by Hurlé and Hinchliffe (1978) concerning the posterior necrotic zone (PNZ) of the chick wing bud: (1) appearance of acid phosphatase-positive autophagic vacuoles in the cytoplasm, (2) increase in size of these vacuoles which leak acid phosphatase activity and become autolytic, (3) cell fragmentation and separation of a large nucleus-containing fragment from the cytoplasm cytolytic fragment, (4)
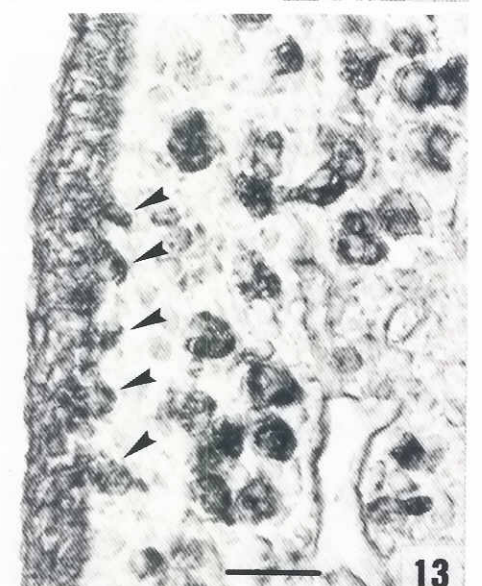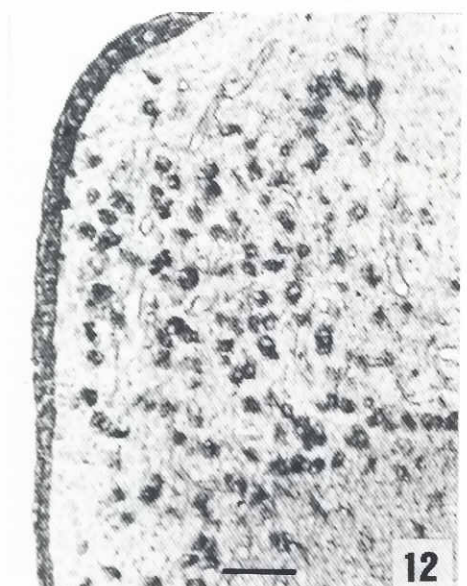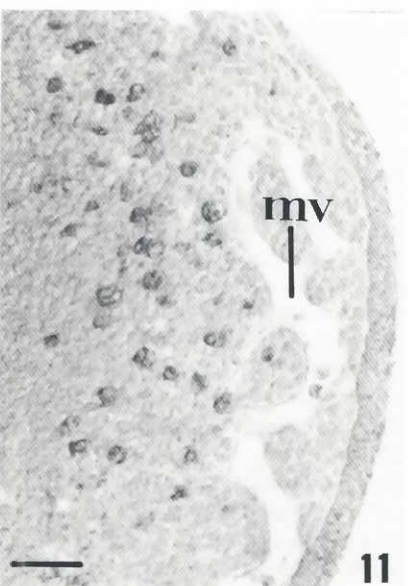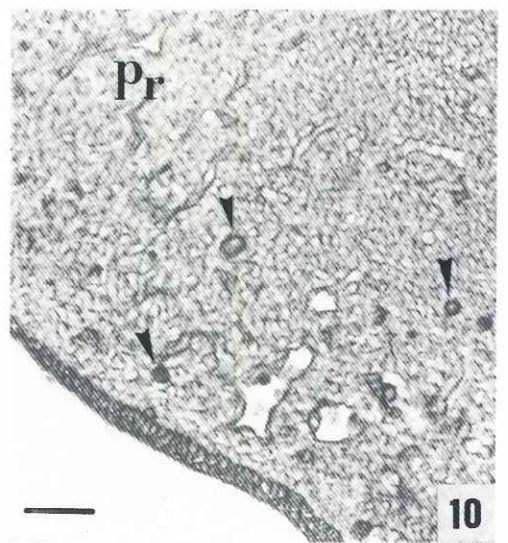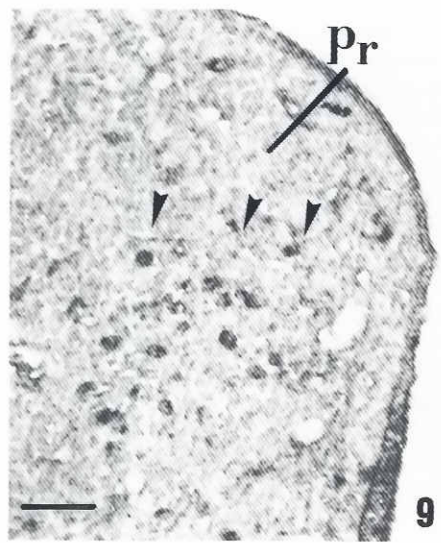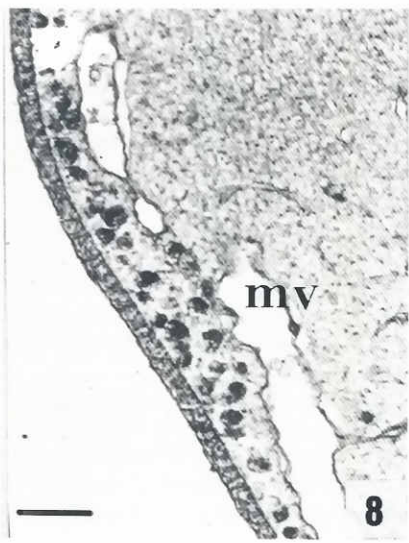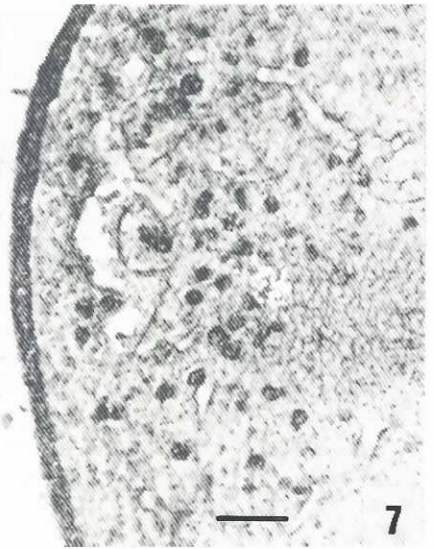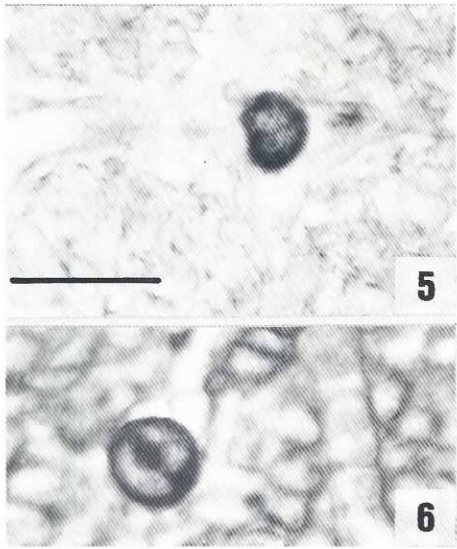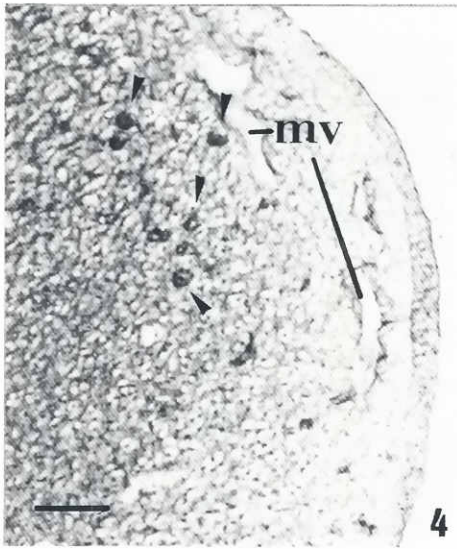
chromatin condensation with further fragmentation of the nucleated part, (5) phagocytosis of fragments by locally differentiating macrophages. Before chromatin condensation, however, the latter concept does not allow a clear distinction, at least at the light microscope level, between primary dying cells and macrophage cells in the early phase of the phagocytic process: both have a normal-looking nucleus and contain cytolytic vacuoles in their cytoplasm. Furthermore, little is known of the mechanism by which macrophage cells identify the cell debris. Several observations from *in vitro* experiments have provided evidence in support of a selective lectin-binding mediated process. Duvall *et al.* (1985) were able to block the binding of macrophages to apoptotic thymocytes by N-acetyl glucosamine. Interestingly, both lectin staining properties demonstrated here in macrophage cells have a selective affinity for that sugar.

In an ultrastructural study on interdigital cell death in chick leg buds, Hurlé and Fernández-Terán (1983) have provided multiple suggestive evidence of the penetration (or outflow?) of macrophage cells into (or from?) the regressing apical ectodermal ridge; in many sites, the epithelial-mesenchymal interface appeared disrupted and lacked the basement membrane, allowing direct contact between mesenchymal cells and basal ectodermal cells. Macrophages were observed (1) under the ectodermal layer establishing close contacts with ectodermal cell processes, (2) partly between the basal ectodermal cells and partly in the mesenchymal space, (3) between basal ectodermal cells, (4) between basal and peridermal ectodermal cells and (5) within the peridermal cell cords detaching into the amniotic cavity. The authors suggest that epithelial cell processes passing through the basal lamina might indicate a phagocytic stimulus to underlying mesodermal cells; these would then differentiate into macrophages, migrate through the epithelial tissue and eventually be detached in the amniotic cavity.

The actual relationship between ectodermal and mesodermal compartments in other areas of superficial cell death are, however, far from being always so obvious. The passage of cell debris from one to the other cell layer has never been suggested in the anterior and posterior necrotic zones of chick limb buds, in spite of the fact that these sites correspond exactly to the areas where the extremities of the a.e.r. have collapsed at earlier stages. Several experimental results support the idea that cell death occurs in the anterior necrotic zone when the morphogen diffused from the zone of polarizing activity slows down below a threshold value (Summerbell, 1979; Hinchliffe and Gumpel-Pinot, 1981). However, no information is available on the possible occurrence of an increased number of dead cells in the anterior ectoderm, which, in turn, might contribute to the increase in the number of phagocytes in the underlying anterior necrotic zone.

Another cause-effect relationship according to which the a.e.r. might influence cell viability in the underlying mesoderm was proposed by Hurlé and Gañán (1986) and by Brewton and MacCabe (1988) on the basis of inhibition of cell death after removal of the adjacent apical ectoderm in chick limb buds. Such interpretation would also become questionable if the degenerative changes demonstrated in the mesoderm were proved to be related to the clearing up of ectodermal debris by mesodermal macrophages.

The observations reported in the present study provide three kinds of evidence for a possible implication of mesenchymal macrophage cells in the clearance of degenerative debris of ectodermal origin: (1) the demonstration of a strict spatial-temporal correspondence between ectodermal and mesodermal necrotic sites, (2) the absence of degenerative changes in the mesoderm surrounding macrophage cells, (3) the accumulation of macrophage cells in the overcrowded *fpp* site of Os/+ limb buds. Of course, the second observation requires ultrastructural confirmation. Electron microscope studies have been undertaken for this purpose and a few preliminary observations concerning early changes in PMNZ of normal hindlimb buds have been obtained. They show the presence of electron dense cellular debris both in the a.e.r. and in the underlying mesoderm. So far, however, we have not detected any disruption of the basement membrane which, however, displays intimate contacts with a number of cytoplasmic protrusions of

---

Fig. 4. Section through the preaxial footplate area of the left hindlimb bud of a normal (+/+) 7.68 mm embryo, N-PNA staining. *N-PNA-positive macrophages (arrowheads) can be seen in the* fpp *site at the borderline between the unstained marginal mesoderm and the positive preskeletal mesoderm. mv: marginal vein (Scale bar, 50 µm)*

Figs. 5 and 6. Binucleated intravascular cells detected in the distal divisions of the axial artery of the hindlimb bud *from embryos with a CR length of 7.57 mm (Fig.5) and 8.70 mm (Fig.6); their cytoplasm exhibits a strong and uniform binding affinity for N-PNA (Scale bar, 25 µm).*

Fig. 7. Section through the preaxial footplate area of the right hindlimb bud of a normal (+/+) 9.14 mm embryo, RCA staining. *Strong RCA binding in the macrophages of the anterior marginal necrotic zone, in the apical ectodermal ridge and in the endothelium of the marginal vein; weak and mainly extracellular staining in the condensed mesoderm of the first digital column. (Scale bar, 50 µm).*

Fig. 8. Section through the postaxial footplate area of the left hindlimb bud of a 9.30mm Xpl/+ embryo, RCA staining. *Strong RCA binding in the macrophages of the posterior marginal necrotic zone, in the apical ectodermal ridge, in the endothelium of the marginal vein (mv) and its affluent vessels; weak and mainly extracellular staining in the condensed mesoderm of the 5th digital column. (Scale bar, 50 µm).*

Figs. 9 and 10. Sections through the preaxial footplate area of the hindlimb bud from two Xpl/+ embryos with a CR length of 8.11 mm (Fig. 9) and 9.30 mm (Fig. 10), RCA staining. *The arrowheads delineate the borderline between the macrophage-free mesoderm of the preaxial protrusion (Pr) and the residual part of the reduced anterior marginal necrotic zone scattered with RCA-positive macrophages. (Scale bar, 50 µm).*

Fig. 11. Section through the preaxial footplate area of the left hindlimb bud of a 7.78mm Os/+ embryo, N-PNA staining. *An excessive number of macrophage cells are present in the* fpp *site lying in a deep location with respect to the marginal vein (mv). (Scale bar, 50 µm).*

Fig. 12. Section through the preaxial footplate area of the right hindlimb bud of a 8.65 mm Os/+ embryo, RCA staining. *An excessive number of macrophage cells are present in the anterior marginal necrotic area; most of them take place anteriorly with respect to the first preskeletal digital ray, which can be seen in the lower right corner of the figure. (Scale bar, 50 µm).*

Fig. 13. Same Os/+ hindlimb bud as in Fig. 12, RCA staining. *Detail of the AMNZ showing numerous RCA-positive macrophage cells in close contact with the basal aspect of the apical ectodermal ridge (arrowheads). (Scale bar, 25 µm).*
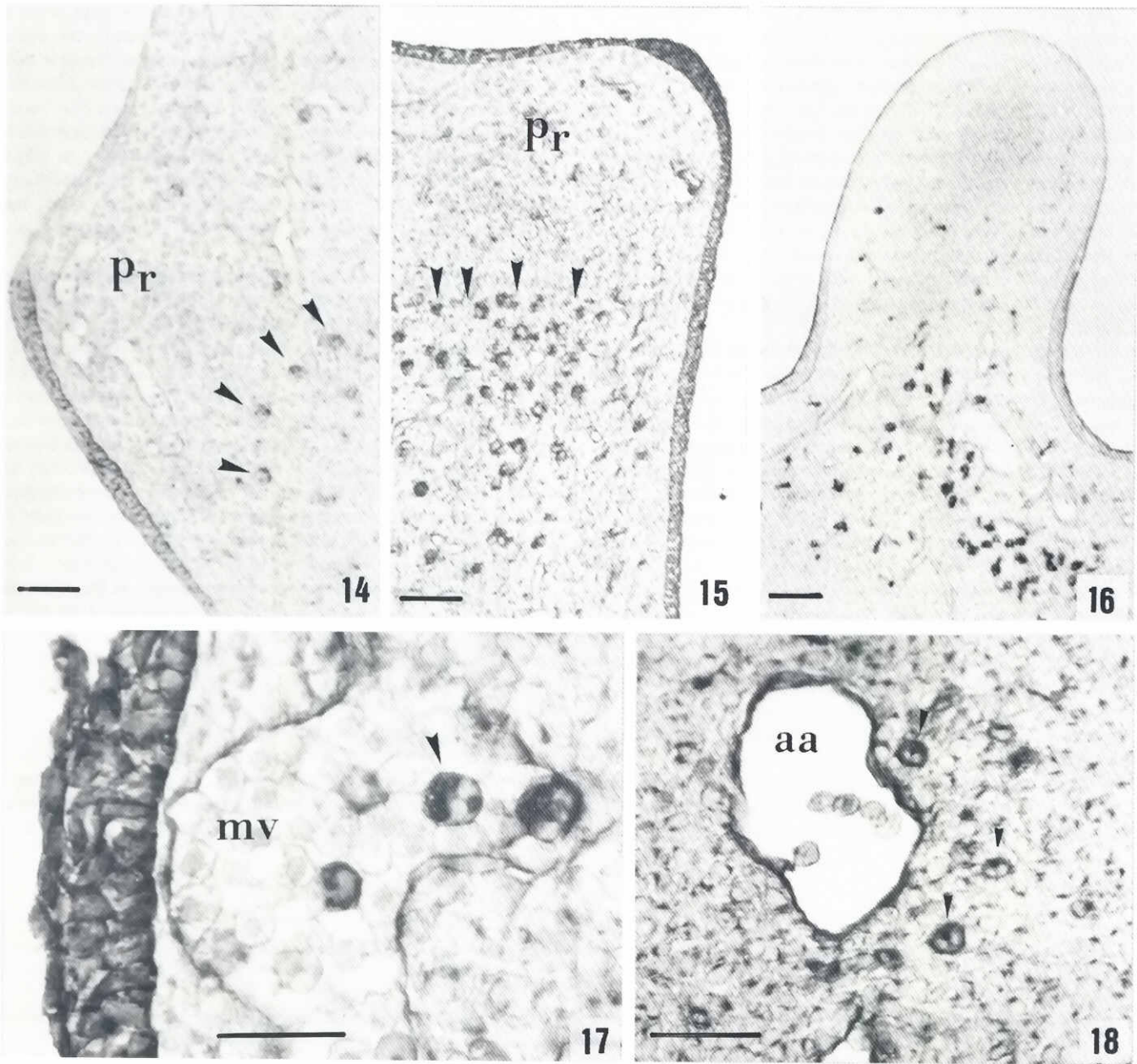
Fig. 14. Section through the preaxial footplate area of the right hindlimb bud of a 7.78 mm Os/+/Xpl/+ hybrid embryo, RCA staining. *The arrowheads delineate the borderline between the macrophage-free mesoderm of the preaxial protrusion (Pr) and the residual fpp site, which has normally disappeared in normal limb buds of similar developmental stage. (Scale bar, 50 μm).*

Fig. 15. Section through the preaxial footplate area of the left hindlimb bud of a 8.54 mm Os/+/Xpl/+ hybrid embryo; RCA staining. *The arrowheads delineate the borderline between the macrophage-free mesoderm of a preaxial protrusion of reduced size and the residual AMNZ territory, in which an excessive number of macrophage cells can be seen; note the strong RCA-staining in the apical ectodermal ridge. (Scale bar, 50 μm).*

Fig. 16. Section through the extra preaxial digital bud of the right hindlimb bud of a 10.5 mm Os/+/Xpl/+ hybrid embryo; RCA staining. *Numerous RCA-positive macrophage cells belonging to the residual AMNZ can be seen at the base of the extra digit. (Scale bar, 50 μm).*

Fig. 17. Detail of the preaxial area of the hindlimb bud footplate of a normal (+/+) 8.27 mm embryo; RCA staining. *Macrophage cells with strongly positive intracytoplasmic inclusions can be seen in the marginal vein (mv); one of them appears obviously binucleated (arrowhead); strong RCA staining in the apical ectodermal ridge and in the vascular endothelium. (Scale bar, 25 μm).*

Fig. 18. Detail of the central area of the left hindlimb bud of a normal (+/+) 7.68 mm embryo; RCA staining. *Strong RCA binding can be seen in the endothelium of the axial artery (aa) and in numerous perivascular binucleated macrophage cells (arrowheads) belonging to the «opaque patch» necrotic site. (Scale bar, 25 μm).*

mesodermal cells, some of which are probably macrophage cells. Before further details can be obtained, the following working hypothesis is proposed: (1) circulating binucleated macrophage cells with strong N-PNA and RCA binding affinities reach the distal mesoderm of the limb bud paddle through the radiating branches of the main artery; (2) after extravasation they migrate and come to lie close to the subectodermal basement membrane in areas of maximal degenerative changes in the adjacent a.e.r.; (3) in a manner which still remains to be clarified, ectodermal cytolytic fragments are transferred from the ectoderm to the underlying macrophage cells; (4) macrophage cells loaded with cellular debris eventually return to the blood stream through the marginal vein or one of its preaxial divisions. The existence of close contacts between the marginal vein and the basement membrane in the preaxial territory probably helps facilitate the transfer of macrophage cells in that area.

Indirect evidence in favor of the above hypothesis can be found in recent observations reported by Kerkhoffs *et al.* (1991) after *in vitro* labeling of mouse embryo ectodermal cells with wheat germ agglutinin conjugated to gold particles. Labeled cells were eventually detected in the mesodermal compartment of the limb buds and might well be macrophage cells loaded with labeled ectodermal fragments. Of course, our hypothesis does not rule out the possible occurrence of simultaneous intrinsic mesodermal cell death in the necrotic sites examined, though the present observations at the optic microscope level did not provide any indication of such feature.

If we try now to apply the new hypothesis to the morphogenetic interpretation of the various teratological situations studied here, a common concept emerges which emphasizes the role of the apical ectoderm in limb development. The absence of cell death in a limited preaxial portion of the a.e.r. observed in several early Xpl/ + limb buds would be the primary cause of the further absence of *fpp* in the underlying mesoderm and of the drastic reduction in the number of macrophages in the preaxial extension of the AMNZ. The occurrence of necrotic changes further posteriorly in the ridge of affected rudiments would of course explain the presence of macrophages in the posterior extension of the AMNZ. Though it could not be ascertained with the staining methods used, a potential increase in the rate of cell death in the preaxial portion of the a.e.r. might logically be responsible for the increased number and advanced appearance of macrophage cells in the *fpp* site of Os/+ limb buds. This interpretation also abolishes the apparent discrepancy between the site of increased macrophage density and the affected territory where the skeletal pattern is eventually modified. The demonstration of degenerative changes in the anterior part of the a.e.r. covering the preaxial protrusion of hybrid Os/+/ Xpl/+ embryos also provides a satisfactory explanation of the pathogenic mechanism leading to the formation of a preaxial protrusion of reduced size. It may be assumed here that the Os and Xpl genes compete to induce in this particular site a rate of ectodermal degeneration which is lower than in Os/+ and +/+ limb buds, though superior to that in the Xpl/+ phenotype. The resulting ectoderm-mesoderm relationship would therefore be compatible with the formation of a reduced preaxial protrusion. Excessive cell death induced in the preaxial a.e.r. by the sole Os gene would be responsible for the accumulation of an excess number of macrophage cells at the posterior border of the overgrown area.

In all abnormal phenotypes examined, the observed or assumed modifications of degenerative phenomena affecting the preaxial part of the a.e.r. may be considered either as intrinsic ectodermal changes or as the consequences of primarily modified ectoderm-mesoderm interactions. Of course, our descriptive analysis cannot provide any evidence in support of one or the other conception.

Materials and Methods

Detailed information on the origin and developmental effects of the mutant genes for oligosyndactylism (Os) and for X-linked polydactyly (Xpl) was given in previous publications (Milaire, 1967b, 1989). For the present study, 73 living embryos collected from 12 litters were obtained by mating heterozygous Os/+ males with Xpl/+ females, the fertility of Xpl/+ males being significantly reduced. Considering the day of vaginal plug discovery as day 0 of gestation, 12, 38, 15 and 8 embryos were collected on day-11, day-12, day-13 and day-18, respectively. The 8 full-term fetuses were submitted *in toto* to alizarin red-alcian blue staining according to the method recommended by Watson (1977) for macroscopic analysis of skeletal defects.

Since a great variety of morphological stages usually coexist among young embryos of similar gestational age, the 65 specimens collected from stages day-11 to day-13 were divided into three groups according to their crown-rump (CR) length. The CR length varies in group 1 from 4.70 to 6.99 mm, in group 2 from 7.00 to 8.99 mm and in group 3 from 9.00 to 10.50 mm. For the most part, the embryos of the first group were sacrificed on day-11, those of the second group on day-12 and those of the third group on day-13. The observations made on day-11 and day-12 in +/+, Xpl/+ and Os/+ limb buds were confirmed or completed by the analysis of 57 additional embryos originating from Xpl/+ x +/+ and from Os/+ x +/+ matings respectively.

Eighty-two embryos of all age groups were submitted for 20 min to supravital staining with Nile blue sulfate (1:40.000 in physiological Locke's solution) at room temperature. After a 15 to 30 minute wash in Locke's solution, the limb buds were dissected out, mounted in hollowed slides and examined extemporaneously under the microscope at low magnification (x32). The patterns of heavily stained necrotic sites were recorded through camera lucida drawings and color photographs.

Twenty-four embryos were fixed by immersion into Serra's solution (95° ethanol, formalin, acetic acid, 6:3:1 volumes) and their isolated limb buds were embedded in Paraplast and cut in two sets of alternating serial sections (8 µm) oriented tangentially to the volar aspects of the foot- or handplate.

Peanut agglutinin binding sites were demonstrated with the Avidin-Biotin-Peroxidase Complex (ABC) procedure, as described in detail in a recent publication (Milaire, 1991).

The isolated limb buds of the remaining 16 embryos have been submitted either to macroscopic examination, or to microscopic analysis of serial sections stained with Pyronin-Methyl green according to Unna-Brachet (Lison, 1953).

References

BREWTON, R.G. and MacCABE, J.A. (1988). Ectodermal influence on physiological cell death in the posterior necrotic zone of the chick wing bud. *Dev. Biol. 126:* 327-330.

CLARKE, P.G.H. (1990). Developmental cell death: morphological diversity and multiple mechanisms. *Anat. Embryol. 181:* 195-213.

DUVALL, E., WYLLIE, A.H. and MORRIS, R.G. (1985). Macrophage recognition of cells undergoing programmed cell death (apoptosis). *Immunology 56:* 351-358.

GRÜNEBERG, H. (1961). Genetical studies on the skeleton of the mouse. XXVII. The development of oligosyndactylism. *Genet. Res., Camb. 2:* 33-42.

HINCHLIFFE, J.R. (1981). Cell death in embryogenesis. In *Cell Death* (Ed. I.D. Bowen and R.A. Lockshin). Chapman and Hall, London, pp. 35-46.

HINCHLIFFE, J.R. and GUMPEL-PINOT, M. (1981). Control of maintenance and anteroposterior skeletal differentiation of the anterior mesenchyme of the chick wing bud by its posterior margin (the ZPA). *J. Embryol. Exp. Morphol. 62:* 63-82.

HURLÉ, J.M. and FERNÁNDEZ-TERÁN, M.A. (1983). Fine structure of the regressing interdigital membranes during the formation of the digits of the chick embryo leg bud. *J. Embryol. Exp. Morphol. 78:* 195-209.

HURLÉ, J.M. and GAÑÁN, Y. (1986). Interdigital tissue chondrogenesis induced by surgical removal of the ectoderm in the embryonic chick leg bud. *J. Embryol. Exp. Morphol. 94:* 231-244.

HURLÉ, J.M. and HINCHLIFFE, J.R. (1978). Cell death in the posterior necrotic zone (PNZ) of the chick wing-bud: a stereoscan and ultrastructural survey of autolysis and cell fragmentation. *J. Embryol. Exp. Morphol. 43:* 123-136.

KERKHOFFS, J-L.H., DE WATER, R., HARTWIG, N.G., VAN IPEREN, L. and VERMEIJ-KEERS, Ch. (1991). The ectodermal cells of the limb bud: source of the mesodermal compartment. *Teratology 44:* 28A.

KLEIN, K.L., SCOTT, W.J. and WILSON, J.G. (1981). Aspirin-induced teratogenesis: a unique pattern of cell death and subsequent polydactyly in the rat. *J. Exp. Zool. 216:* 107-112.

LISON, L. (1953). *Histochemie et Cytochimie Animales.* Gauthier Villars, Paris, pp. 281-300.

MILAIRE, J. (1965). Etude morphogénétique de trois malformations congénitales de l'autopode chez la souris (syndactylisme-brachypodisme-hémimélie dominante) par des méthodes cytochimiques. *Acad. R. Belg. Cl. Sci., Mém. in 4° (Sc.) 16:* 1-120.

MILAIRE, J. (1967a). Evolution des processus dégénératifs dans la cape apicale au cours du développement des membres chez le rat et la souris. *C.R. Acad. Sci. Paris 265:* 137-140.

MILAIRE, J. (1967b). Histochemical observations on the developing foot of normal, oligosyndactylous (Os/+) and syndactylous (sm/sm) mouse embryos. *Arch. Biol. (Liège) 78:* 223-288.

MILAIRE, J. (1971). Evolution et déterminisme des dégénérescences cellulaires au cours de la morphogenèse des membres et leurs modifications dans diverses situations tératologiques. In *Malformations Congénitales des Mammifères* (Ed. H. Tuchmann-Duplessis). Masson et Co., Paris, pp. 131-149.

MILAIRE, J. (1976). Rudimentation digitale au cours du développement normal de l'autopode chez les mammifères. In *Mécanismes de la Rudimentation des Organes chez les Embryons des Vertébrés* (Ed. A. Raynaud). Editions du C.N.R.S., Paris, pp. 221-233.

MILAIRE, J. (1989). Development of X-linked polydactyly in the mouse. I. Analysis of the malformations in embryos and full term fetuses. *Arch. Biol. (Bruxelles) 100:* 353-382.

MILAIRE, J. (1991). Lectin binding sites in developing mouse limb buds. *Anat. Embryol. 184:* 479-488.

MILAIRE, J. and ROOZE, M. (1983). Hereditary and induced modifications of the normal necrotic patterns in the developing limb buds of the rat and mouse: facts and hypotheses. *Arch. Biol. (Bruxelles) 94:* 459-490.

NARUSE, I. and KAMEYAMA, Y. (1986). Prevention of genetic polydactyl in Polydactyly Nagoya (Pdn) mice *in vitro* by surgical treatment of footplate during embryogenesis. *Congenital Anomalies 26:* 1-9.

SCHWEICHEL, J.U. and MERKER, H.J. (1973). The morphology of various types of cell death in prenatal tissues. *Teratology 7:* 253-266.

SCOTT, W.J. (1981). Pathogenesis of bromodeoxyuridine induced polydactyl. *Teratology 23:* 383-389.

SCOTT, W.J., RITTER, E.J. and WILSON, J.G. (1977). Delayed appearance of ectodermal cell death as a mechanism of polydactyly induction. *J. Embryol. Exp. Morphol. 42:* 93-104.

SCOTT, W.J., RITTER, E.J. and WILSON, J.G. (1980). Ectodermal and mesodermal cell death patterns in 6-mercaptopurine riboside-induced digital deformities. *Teratology 21:* 271-279.

SKALKO, R.G., PERRINS, N.M. and NILES, A.M. (1977). The effect of 5-bromodeoxyuridine on mouse limb development. *Acta Embryol. Exp. 3:* 323-333.

SUMMERBELL, D. (1979). The zone of polarizing activity, evidence for a role in normal chick morphogenesis. *J. Embryol. Exp. Morphol. 50:* 217-233.

WATSON, A.G. (1977). *In toto* alcian blue staining of the cartilaginous skeleton in mammalian embryos. *Anat. Rec. 187:* 743.

WYLLIE, A.H., KERR, J.F.R. and CURRIE, A.R. (1980) Cell death: the significance of apoptosis. *Int. Rev. Cytol. 68:* 251-306.